

Graphite-Conjugated Rhenium Catalysts for Carbon Dioxide Reduction

Seokjoon Oh,[†] James R. Gallagher,[‡] Jeffrey T. Miller,^{‡,§} and Yogesh Surendranath^{*,†}

[†]Department of Chemistry, Massachusetts Institute of Technology, Cambridge, Massachusetts 02139, United States

[‡]Chemical Science and Engineering Division, Argonne National Laboratory, Argonne, Illinois 60439, United States

[§]School of Chemical Engineering, Purdue University, West Lafayette, Indiana 47907, United States

S Supporting Information

ABSTRACT: Condensation of *fac*-Re(5,6-diamino-1,10-phenanthroline)(CO)₃Cl to *o*-quinone edge defects on graphitic carbon surfaces generates graphite-conjugated rhenium (GCC-Re) catalysts that are highly active for CO₂ reduction to CO in acetonitrile electrolyte. X-ray photoelectron and X-ray absorption spectroscopies establish the formation of surface-bound Re centers with well-defined coordination environments. GCC-Re species on glassy carbon surfaces display catalytic currents greater than 50 mA cm⁻² with 96 ± 3% Faradaic efficiency for CO production. Normalized for the number of Re active sites, GCC-Re catalysts exhibit higher turnover frequencies than that of a soluble molecular analogue, *fac*-Re(1,10-phenanthroline)(CO)₃Cl, and turnover numbers greater than 12,000. In contrast to the molecular analogue, GCC-Re surfaces display a Tafel slope of 150 mV/decade, indicative of a catalytic mechanism involving rate-limiting one-electron transfer. This work establishes graphite-conjugation as a powerful strategy for generating well-defined, tunable, heterogeneous electrocatalysts on ubiquitous graphitic carbon surfaces.

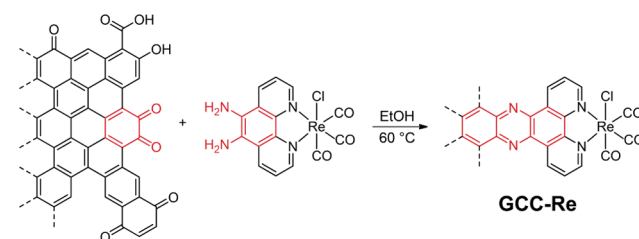
The catalytic interconversion of electricity and fuel is an attractive method for integrating intermittent renewable energy sources such as solar and wind into the current energy infrastructure. This interconversion is catalyzed at the surfaces of extended solids¹ or via redox mediation at molecular active sites.² Whereas molecular catalysts can be tuned synthetically to optimize the kinetics and/or thermodynamics of substrate activation,^{3,4} electrode surfaces typically consist of a distribution of active sites that are difficult to modify at the molecular level.⁵ However, surface catalysts are more readily integrated into energy conversion devices such as fuel cells and electrolyzers and often exhibit greater stability than their molecular counterparts. Thus, methods for constructing molecularly well-defined, tunable surface catalysts that capture the advantages of both systems are highly desirable.

There are numerous methods for immobilizing molecular catalysts onto electrode surfaces, ranging from those that utilize weak physisorption/electrostatic interactions^{6,7} to those that form strong covalent linkages.^{8–10} However, with rare exceptions,¹¹ these methods connect the catalytic unit to the electrode surface through inert tethers that engender weak electronic coupling between the molecular active site and the

delocalized states of the metallic electrode. In contrast, the active sites on metal surfaces are strongly coupled to the band states of the solid, and such interactions have been shown to facilitate substrate activation.¹²

Herein, we develop a simple surface functionalization strategy for conjugating transition-metal active sites to carbon surfaces by exploiting the native surface chemistry of graphite. In a prior report, we demonstrated that *o*-quinone moieties found commonly on graphite edge planes¹³ condense site-selectively with *o*-phenylenediamines under mild conditions, producing well-defined graphite-conjugated catalysts (GCCs) that display high activity for the oxygen reduction reaction in alkaline aqueous electrolytes.¹⁴ In this work, we show that this surface functionalization strategy can be readily applied to generate well-defined, highly active, transition-metal-based surface electrocatalysts (Scheme 1).

Scheme 1. Synthesis of GCC-Re Active Sites



We targeted GCCs bearing *fac*-Re(1,10-phenanthroline)(CO)₃Cl (Re(phen)(CO)₃Cl) fragments as a model system. Re coordination compounds of this general form are known catalysts for carbon dioxide reduction (CDR) to CO^{3,15} and have been immobilized onto electrode surfaces via electropolymerization^{9,10} and adsorption on polymeric¹⁶ and graphitic surfaces.⁷ Although all three strategies generate active electrodes, surface adsorption has led to low catalyst lifetimes, and the poor conductivity of polymeric films introduces severe limitations on electron transport. Additionally, electropolymerization generates a complex distribution of Re sites consisting of Re–Re bonded dimers and Re–C linkages that are catalytically inert.⁹ As a result, prior efforts at immobilization have generally failed to reproduce the activity and/or selectivity of the discrete molecular species. Herein we show that graphite-conjugated rhenium (GCC-Re)

Received: December 14, 2015

Published: January 23, 2016

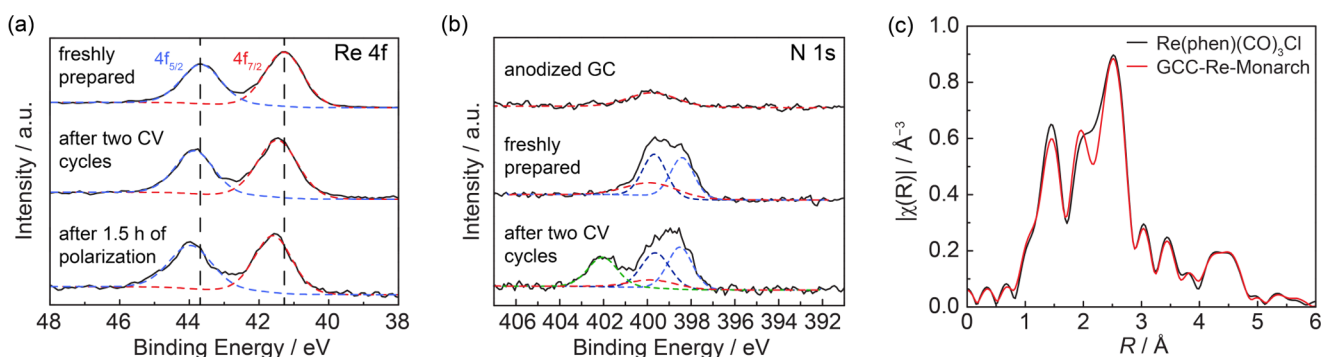


Figure 1. (a) High-resolution Re 4f XPS spectra of freshly prepared GCC-Re (top), GCC-Re following two CV cycles (middle), and GCC-Re following 1.5 h of cathodic electrolysis at 1.0 mA cm^{-2} (bottom). (b) High-resolution N 1s XPS spectra of an oxidized GC electrode (top), freshly prepared GCC-Re (middle), and GCC-Re following two CV cycles (bottom). (c) k^2 -weighted magnitude of the Fourier transform of the extended X-ray absorption fine structure ($\Delta k = 2.6\text{--}11.9 \text{ \AA}^{-1}$) of $\text{Re}(\text{phen})(\text{CO})_3\text{Cl}$ (black) and GCC-Re modified Monarch 1300 (Red). The imaginary parts of the Fourier transform (not shown) of $\text{Re}(\text{phen})(\text{CO})_3\text{Cl}$ and GCC-Re modified Monarch carbon powder are also identical.

surfaces display a uniform distribution of well-defined Re sites that perform CO_2 reduction to CO with near-unity selectivity and improved activities relative to that of a soluble molecular analogue.

To facilitate detailed electrochemical studies, we prepared GCC-Re as described in Scheme 1 using a glassy carbon (GC) electrode as the graphitic host. GCC-Re refers to this functionalized GC surface unless otherwise noted. To clean the GC surface and increase the population of *o*-quinone moieties, electrodes were subjected to a brief anodic treatment adapted from literature methods.¹⁷ The oxidized GC electrodes were then treated with $\text{Re}(5,6\text{-diamino-1,10-phenanthroline})(\text{CO})_3\text{Cl}$ in ethanol for 12 h at $60 \text{ }^\circ\text{C}$ (Scheme 1). Residual monoimine-linked and physisorbed $\text{Re}(5,6\text{-diamino-1,10-phenanthroline})(\text{CO})_3\text{Cl}$ was removed by subsequent treatment with 0.1 M HCl followed by washing with copious amounts of water and ethanol, furnishing the final GCC-Re surface.

Surface analysis supports the structural assignment shown in Scheme 1 for GCC-Re. Survey XPS spectra of GCC-Re (Figure S2) exhibit new peaks corresponding to Re 4f and Cl 3p transitions as well as increased intensity in the N 1s peak relative to the native N concentration of unmodified GC electrodes. Peak integrations reveal an increase in atomic surface concentrations of 1.2 and 4.2% for Re and N, respectively (Table S1), consistent with the expected Re/N ratio of 1:4 based on the structure of GCC-Re. High-resolution XPS spectra provide additional information about the surface chemistry of the modified electrodes. The Re 4f spectrum of freshly prepared GCC-Re (Figure 1a, top) reveal Re $4f_{5/2}$ and $4f_{7/2}$ peaks at 43.7 and 41.3 eV, respectively. These peaks are sharp, with full widths at half-maximum (fwhm) of 1.29 and 1.34 eV, respectively, indicating the presence of a single homogeneous environment for the Re centers. Likewise, the N 1s spectra of freshly prepared GCC-Re (Figure 1b, middle) evince the introduction of two new surface nitrogen environments above the native N background of the unmodified electrode (Figure 1b, top). The new peaks appear in a 1:1 ratio at 398.4 and 399.7 eV corresponding to the pyrazine and phenanthroline nitrogens, respectively.^{14,18} Together, the XPS data support the formation of discrete $\text{Re}(\text{phen})(\text{CO})_3\text{Cl}$ fragments linked to the surface through pyrazine bridges in GCC-Re.

X-ray absorption spectroscopy (XAS) provides additional evidence in support of the existence of molecularly well-defined Re centers on GCC-Re surfaces. To facilitate XAS studies, high surface area Monarch 1300 carbon black was used as the support

instead of GC. Application of the same synthetic method in Scheme 1 generates GCC-Re modified Monarch carbon with a 1.8 wt % Re loading as determined by inductively coupled plasma optical emission spectrometry. Re L_3 -edge X-ray absorption near edge spectroscopy (XANES) of GCC-Re modified Monarch carbon and $\text{Re}(\text{phen})(\text{CO})_3\text{Cl}$ reveal nearly identical spectra (Figure S1), establishing no significant changes in the oxidation state or local coordination geometry of the Re centers upon surface condensation. In addition, extended X-ray absorption fine structure (EXAFS) spectra of both samples (Figure 1c) reveal excellent agreement, indicating that the local environment of the Re center remains unchanged upon condensation. Together, XPS and XAS establish that this mild surface ligation strategy preserves the integrity of the Re sites.

GCC-Re catalysts display high activity for CO_2 reduction to CO. The cyclic voltammogram (CV) of GCC-Re recorded in CO_2 -saturated acetonitrile (MeCN) containing 0.1 M tetrabutylammonium hexafluorophosphate (TBAPF_6) electrolyte (Figure 2, red solid line) displays a large catalytic wave that reaches 10 mA cm^{-2} at -2.09 V (all potentials are reported versus the ferrocene/ferrocenium couple and normalized to the geometric surface area of the electrode) corresponding to CDR catalysis. No catalytic current was observed for GCC-Re in the absence of CO_2 (Figure 2, black dashed line). Both GC electrodes modified

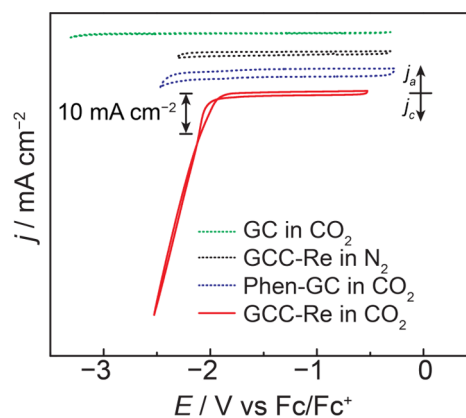


Figure 2. Cyclic voltammograms (100 mV/s scan rate, 1000 rpm rotation rate) of GCC-Re (red), 5,6-diamino-1,10-phenanthroline treated GC (blue), and unmodified GC (green) electrodes recorded in CO_2 -saturated 0.1 M TBAPF_6 MeCN electrolyte. CV of GCC-Re in N_2 -saturated 0.1 M TBAPF_6 MeCN electrolyte (black).

with 5,6-diamino-1,10-phenanthroline without the Re center (Figure 2, blue dashed line) and unmodified GC electrodes (Figure 2, green dashed line) did not display CDR catalysis over the same potential range in CO₂-saturated MeCN. Likewise, no catalytic current was observed for GCC-Re in the absence of CO₂ (Figure 2, black dashed line). Notably, discrete redox waves corresponding to Re or phen reduction are not observed for GCC-Re despite the observation of a strong catalytic current.

GCC-Re surface sites remain robust under the conditions of catalysis, but the GC host surface is subject to dynamic change upon initial polarization. The CV scan of GCC-Re in Figure 2 remains unchanged upon subsequent scanning but differs from the initial trace recorded on a freshly prepared GCC-Re electrode. The initial CV scan (Figure S3) displays a broad cathodic feature spanning from -0.80 to -2.06 V. This feature is also observed for the unmodified oxidized GC electrode and is attributed to detachment of loosely bound graphitic domains or graphene sheets on the oxidized GC surface. This contention is corroborated by reports of reductive exfoliation of graphene induced by tetrabutylammonium cation intercalation into graphite.¹⁹ Indeed, XPS spectra recorded following polarization display a new N 1s peak at 402.0 eV, corresponding to tetraalkylammonium ions (Figure 1b).²⁰ Inductively coupled plasma mass spectrometry (ICP-MS) quantification (Table S2) reveals a decrease in surface Re concentration following the initial CV cycles of a freshly prepared GCC-Re electrode, in line with partial detachment of graphitic domains from the surface. However, after this initial loss, Re surface concentrations remained stable during CV cycling.

Superimposed on the broad cathodic feature in the initial CV scan is a sharp irreversible wave at -1.61 V that we attribute to reductive cleavage of the Re-Cl bond (Figure S3). This assignment is also supported by XPS spectra recorded following two CV scans of a freshly prepared GCC-Re electrode, which reveal significantly diminished Cl surface concentrations (Table S1) and Re 4f peaks that are shifted positively by 0.3 eV (Figure 1a). The positive shift of the Re 4f peaks is consistent with exchange of Cl for more electron-withdrawing CO generated during catalysis. We note that Cl dissociation has been documented for analogous molecular species at similar potentials.^{15d} However, the Re 4f peaks remain sharp (fwhm = 1.45 and 1.27 eV) following CV scans over the catalytic wave, indicating that the Re center is not subject to degradation on the time scale of the measurement. Likewise, no peaks are observed at ~40.3 eV expected for the Re 4f_{7/2} peak of Re⁰, excluding significant formation of metallic Re nanoparticles.²¹ Additionally, high-resolution XPS spectra of the N 1s region (Figure 1b) reveal that the pyrazine and phenanthroline peaks at 398.4 and 399.7 eV persist even after reductive polarization into the catalytic wave. Together, the data suggest that surface bound Re centers remain robust under the conditions of CDR catalysis.

GCC-Re is highly selective for CO₂ reduction to CO. The gaseous products of CDR catalysis were analyzed in real-time by in-line gas chromatography. The GCC-Re modified electrodes were polarized at constant cathodic current densities of 0.50 and 1.0 mA cm⁻² in gastight electrochemical cells that were continuously sparged with CO₂. CO was the only product detected by gas chromatography and was produced with a Faradaic efficiency (FE) of 96 ± 3%, indicating that GCC-Re modified electrodes retain the high selectivity for CO production observed for homogeneous molecular analogs.

To gain insight into the mechanism of CDR catalyzed by GCC-Re, we examined steady-state catalytic activity using

galvanostatic measurements. The steady-state currents were normalized to the surface concentration of Re, as determined by ICP-MS (Table S2), to calculate lower limit turnover frequencies (TOFs) expressed in units of CO produced per Re site per second. The Re concentration of GCC-Re after two CV cycles (2.1 nmol cm⁻²) was used to provide an upper limit estimate of the surface active site population. The Tafel data (Figure 3) exhibit linearity over an ~0.6 V range and display a Tafel slope for GCC-Re of ~150 mV/decade, suggesting that catalysis is gated by a rate-limiting one-electron transfer.

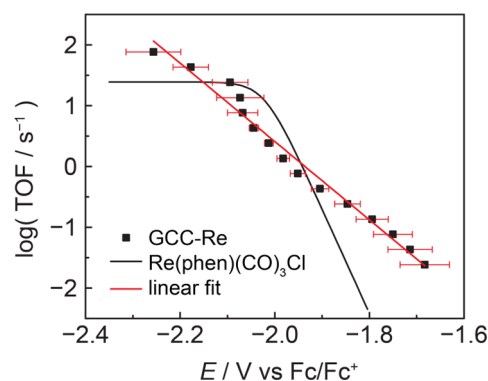


Figure 3. Tafel plots of turnover frequency versus potential for CO₂ reduction catalysis by GCC-Re (black squares) Re(phen)CO₃Cl (solid black line). Data for GCC-Re are the average and standard deviation of four independently prepared electrodes. The slope of a linear fit to the Tafel data (red line) is 150 mV/decade.

The TOFs of GCC-Re are greater than that of the molecular Re(phen)CO₃Cl catalyst across a wide range of potentials. The CV scans of freely diffusing Re(phen)CO₃Cl (Figure S4) display classical S-shaped catalytic waves, which were examined by foot-of-the-wave analysis (see SI for details).²² The resulting TOF data for the molecular catalyst are overlaid with that of GCC-Re in Figure 3. As the Re(phen)CO₃Cl proceeds via an EC mechanism, its catalytic activity scales by 60 mV/decade at potentials more positive than the catalytically relevant Re^{+1/0} redox potential of -2.0 V and is invariant at potentials more negative than -2.0 V. The higher Tafel slope observed for GCC-Re suggests that surface conjugation induces a change in mechanism, leading to higher observed activity at the lowest overpotentials and no clear plateau at high overpotentials. We stress that the TOFs observed for GCC-Re are lower limit values that may be suppressed due to local depletion of CO₂ on the roughened GC surface or transient deactivation of catalytic sites, both of which are explicitly excluded in foot-of-the-wave analysis of molecular electrocatalysts. Together, the data establish that the surface modification method described here is effective for translating the robust activity of Re-based CDR catalysts to carbon surfaces.

Previous attempts at immobilizing Re-based CDR catalysts via adsorption or electropolymerization rarely report stability data. Relative to the few reports of catalyst stability,^{7,9,10} GCC-Re exhibits superior durability. Controlled current electrolyses of GCC-Re (Figure S6) reveal sustained catalytic activity at 1.0 mA cm⁻² (corresponding to a TOF of 2.5 s⁻¹) for 1.4 ± 0.3 h followed by rapid deactivation. Using the Re concentration on a GCC-Re surface after two CV cycles, this corresponds to a lower-limit per Re turnover number (TON) of 12,000, significantly greater than the best literature report of 3800 for a Re, Ru copolymer film.⁹ Similar TONs are observed for constant

potential electrolyses (Figure S8). While the deactivation mechanism is still the subject of ongoing study, Re XPS spectra recorded following 1.4 h electrolyses indicate negligible change in Re 4f peak positions or widths (Figure 1a), suggesting that the Re centers retain their structure and valency. Notably, CV cycling GCC-Re between -0.2 and -2.1 V following 2 h of galvanostatic polarization recovers significant catalytic activity (Figure S7), suggesting that electrode deactivation may be due to the formation of a passivating film on the electrode, which is removed upon polarization at anodic potentials.

In summary, we report the facile preparation of catalytically active graphitic carbon surfaces via condensation of *fac*-Re(5,6-diamino-1,10-phenanthroline)(CO)₃Cl complexes with surface *o*-quinone moieties. The resulting GCC-Re surfaces consist of a uniform array of Re centers with well-defined local coordination environments that are active for CO₂ reduction to CO with near quantitative Faradaic efficiencies and TOFs that exceed that of a homogeneous molecular analogue. GCC-Re surfaces display a Tafel slope of ~ 150 mV/dec, suggesting that graphite-conjugation alters the mechanism of catalysis while preserving high rates of substrate activation. Additionally, this simple, irreversible surface ligation chemistry affords improved catalyst durability relative to adsorption or electropolymerization methods for preparing immobilized catalysts. Given the plethora of known polypyridyl coordination compounds, these results open the door to the systematic study of modified electrodes with well-defined, tunable, metal-based active sites for a wide array of energy conversion reactions.

■ ASSOCIATED CONTENT

Supporting Information

The Supporting Information is available free of charge on the ACS Publications website at DOI: 10.1021/jacs.5b13080.

Full experimental details, XANES and survey XPS spectra, GCC-Re surface Re concentrations, additional voltammograms, foot-of-the-wave analysis details, and galvanostatic polarization traces (PDF)

■ AUTHOR INFORMATION

Corresponding Author

*yogi@mit.edu

Notes

The authors declare no competing financial interest.

■ ACKNOWLEDGMENTS

This research was funded by the U.S. Department of Energy, Office of Science, Office of Basic Energy Sciences, under award number DE-SC0014176 and by the MIT Department of Chemistry through junior faculty funds for Y.S. Additionally, S.O. was supported by the National Science Foundation Graduate Research Fellowship under Grant No. 1122374. J.R.G. and J.T.M. were supported by the U.S. Department of Energy, Office of Basic Energy Sciences, Chemical Sciences under Contract DE-AC-02-06CH11357. Use of the Advanced Photon Source is supported by the U.S. Department of Energy, Office of Science, and Office of Basic Energy Sciences, under Contract DE-AC02-06CH11357. Materials Research Collaborative Access Team (MRCAT, Sector 10 BM) operations are supported by the Department of Energy and the MRCAT member institutions.

■ REFERENCES

- (1) (a) Hori, Y. In *Modern Aspects of Electrochemistry*; Vayenas, C. G., White, R. E., Gamboa-Aldeco, M. E., Eds.; Springer: New York, 2008; Vol. 42, pp 89–189. (b) Li, C. W.; Ciston, J.; Kanan, M. W. *Nature* **2014**, *508*, 504. (c) Falkowski, J. M.; Concannon, N. M.; Yan, B.; Surendranath, Y. *J. Am. Chem. Soc.* **2015**, *137*, 7978.
- (2) Savéant, J.-M. *Chem. Rev.* **2008**, *108*, 2348.
- (3) Smieja, J. M.; Kubiak, C. P. *Inorg. Chem.* **2010**, *49*, 9283.
- (4) (a) O'Hagan, M.; Shaw, W. J.; Raugei, S.; Chen, S.; Yang, J. Y.; Kilgore, U. J.; Dubois, D. L.; Bullock, R. M. *J. Am. Chem. Soc.* **2011**, *133*, 14301. (b) Matson, B. D.; Carver, C. T.; Von Ruden, A.; Yang, J. Y.; Raugei, S.; Mayer, J. M. *Chem. Commun.* **2012**, *48*, 11100. (c) Agarwal, J.; Shaw, T. W.; Stanton, C. J.; Majetich, G. F.; Bocarsly, A. B.; Schaefer, H. F. *Angew. Chem., Int. Ed.* **2014**, *53*, 5152.
- (5) Feng, X.; Jiang, K.; Fan, S.; Kanan, M. W. *J. Am. Chem. Soc.* **2015**, *137*, 4606.
- (6) Mann, J. A.; Rodríguez-López, J.; Abruña, H. D.; Dichtel, W. R. *J. Am. Chem. Soc.* **2011**, *133*, 17614.
- (7) Blakemore, J. D.; Gupta, A.; Warren, J. J.; Brunshwig, B. S.; Gray, H. B. *J. Am. Chem. Soc.* **2013**, *135*, 18288.
- (8) (a) Devadoss, A.; Chidsey, C. E. D. *J. Am. Chem. Soc.* **2007**, *129*, 5370. (b) Yao, S. A.; Ruther, R. E.; Zhang, L.; Franking, R. A.; Hamers, R. J.; Berry, J. F. *J. Am. Chem. Soc.* **2012**, *134*, 15632. (c) Bélanger, D.; Pinson, J. *Chem. Soc. Rev.* **2011**, *40*, 3995. (d) Sheridan, M. V.; Lam, K.; Geiger, W. E. *J. Am. Chem. Soc.* **2013**, *135*, 2939.
- (9) O'Toole, T. R.; Sullivan, B. P.; Bruce, M. R.-M.; Margerum, L. D.; Murray, R. W.; Meyer, T. J. *J. Electroanal. Chem. Interfacial Electrochem.* **1989**, *259*, 217.
- (10) Cabrera, C. R.; Abruña, H. D. *J. Electroanal. Chem. Interfacial Electrochem.* **1986**, *209*, 101.
- (11) McCrory, C. C. L.; Devadoss, A.; Ottenwaelder, X.; Lowe, R. D.; Stack, T. D. P.; Chidsey, C. E. D. *J. Am. Chem. Soc.* **2011**, *133*, 3696.
- (12) (a) Santos, E.; Schmickler, W. *ChemPhysChem* **2006**, *7*, 2282. (b) Nørskov, J. K.; Bligaard, T.; Rossmeisl, J.; Christensen, C. H. *Nat. Chem.* **2009**, *1*, 37.
- (13) (a) Thorogood, C. A.; Wildgoose, G. G.; Crossley, A.; Jacobs, R. M. J.; Jones, J. H.; Compton, R. G. *Chem. Mater.* **2007**, *19*, 4964. (b) McCreery, R. L. *Chem. Rev.* **2008**, *108*, 2646.
- (14) Fukushima, T.; Drisdell, W.; Yano, J.; Surendranath, Y. *J. Am. Chem. Soc.* **2015**, *137*, 10926.
- (15) (a) Hawecker, J.; Lehn, J.-M.; Ziessel, R. *J. Chem. Soc., Chem. Commun.* **1984**, 328. (b) Sullivan, B. P.; Bolinger, C. M.; Conrad, D.; Vining, W. J.; Meyer, T. J. *J. Chem. Soc., Chem. Commun.* **1985**, 1414. (c) Breikss, A. I.; Abruña, H. D. *J. Electroanal. Chem. Interfacial Electrochem.* **1986**, *201*, 347. (d) Johnson, F. P. a; George, M. W.; Hartl, F.; Turner, J. J. *Organometallics* **1996**, *15*, 3374. (e) Keith, J. A.; Grice, K. A.; Kubiak, C. P.; Carter, E. A. *J. Am. Chem. Soc.* **2013**, *135*, 15823.
- (16) Yoshida, T.; Tsutsumida, K.; Teratani, S.; Yasufuku, K.; Kaneko, M. *J. Chem. Soc., Chem. Commun.* **1993**, 631.
- (17) Engstrom, R. C.; Strasser, V. A. *Anal. Chem.* **1984**, *56*, 136.
- (18) Brisdon, B. J.; Griffin, G. F.; Pierce, J.; Walton, R. A. *J. Organomet. Chem.* **1981**, *219*, 53.
- (19) (a) Cooper, A. J.; Wilson, N. R.; Kinloch, I. a.; Dryfe, R. a. W. *Carbon* **2014**, *66*, 340. (b) Cooper, A. J.; Velický, M.; Kinloch, I. A.; Dryfe, R. A. W. *J. Electroanal. Chem.* **2014**, *730*, 34.
- (20) Sieklucka, B.; Dziembaj, R.; Witkowski, S. *Inorg. Chim. Acta* **1991**, *187*, 5.
- (21) Fukuda, Y.; Honda, F.; Wayne Rabalais, J. *Surf. Sci.* **1980**, *93*, 338.
- (22) Costentin, C.; Savéant, J.-M. *ChemElectroChem* **2014**, *1*, 1226.

■ NOTE ADDED AFTER ASAP PUBLICATION

This article was published ASAP on February 4, 2016 with inaccurate corrections due to production error. The corrected paper reposted on February 5, 2016.